Polycomb suppresses a female gene regulatory network to ensure testicular differentiation

So Maezawa[1, 2, 3, 4*], Masashi Yukawa[2, 5, 9], Kazuteru Hasegawa[1, 2, 10], Ryo Sugiyama[3], Mengwen Hu[1, 2, 6], Miguel Vidal[7], Haruhiko Koseki[8], Artem Barski[2, 5], Tony DeFalco[1, 2], and Satoshi H. Namekawa[1, 2, 6*]

[1] Division of Reproductive Sciences, Division of Developmental Biology, Perinatal Institute, Cincinnati Children's Hospital Medical Center, Cincinnati, Ohio, 45229, USA

[2] Department of Pediatrics, University of Cincinnati College of Medicine, Cincinnati, Ohio, 45229, USA

[3] Department of Animal Science and Biotechnology, School of Veterinary Medicine, Azabu University, Sagamihara, Kanagawa 252-5201, Japan

[4] Faculty of Science and Technology, Department of Applied Biological Science, Tokyo University of Science, Chiba 278-8510, Japan.

[5] Division of Allergy and Immunology, Division of Human Genetics, Cincinnati Children's Hospital Medical Center, Cincinnati, Ohio, 45229, USA

[6] Department of Microbiology and Molecular Genetics, University of California, Davis, California, 95616, USA

[7] Centro de Investigaciones Biológicas Margarita Salas, Department of Cellular and Molecular Biology, Madrid 28040, Spain

[8] Developmental Genetics Laboratory, RIKEN Center for Allergy and Immunology, Yokohama, Kanagawa, Japan

[9] Present address: Department of Chemical Pathology, The Chinese University of Hong Kong, Prince of Wales Hospital, Sha Tin, New Territories, Hong Kong

25 [10] Present address: Stanford Cancer Institute, Stanford University School of Medicine, Stanford,

26 CA 94305, USA

27

28 [*]Correspondence: E-mail: s-maezawa@rs.tus.ac.jp; snamekawa@ucdavis.edu

Abstract

Gonadal sex determination is controlled by the support cells of testes and ovaries. In testes, the epigenetic mechanism that maintains cellular memory to suppress female sexual differentiation remains unknown. Here, we show that Polycomb suppresses a female gene regulatory network in Sertoli cells, the specific support cells for postnatal testes. Through genetic ablation, we removed Polycomb repressive complex 1 (PRC1) from embryonic Sertoli cells after sex determination. PRC1-depleted postnatal Sertoli cells exhibited defective proliferation and cell death, leading to the degeneration of adult testes. In adult Sertoli cells, PRC1 suppressed the specific, critical genes required for granulosa cells, the support cells of ovaries, thereby inactivating the female gene regulatory network. The underlying chromatin of female genes was coated with Polycomb-mediated repressive modifications: PRC1-mediated H2AK119ub and PRC2-mediated H3K27me3. Taken together, we identify a critical mechanism centered on Polycomb that maintains the male fate in adult testes.

Introduction

In mammals, gonadal sex determination takes place in the bipotential somatic cell precursors of male Sertoli cells and female granulosa cells in embryos (Capel, 2017; Swain & Lovell-Badge, 1999; Wilhelm, Palmer, & Koopman, 2007). Sertoli cells are the first somatic cells to differentiate in the XY gonad. In testes, Sertoli cells function as a regulatory hub for both differentiation and survival of germ cells, thereby determining male sexual fate (Svingen & Koopman, 2013). The mechanisms maintaining the male cellular identity of Sertoli cells are fundamental for adult testicular functions, including spermatogenesis and hormone production.

At the time of sex determination in embryos, the commitment to the male fate is triggered by the expression of the Y-linked *Sry* gene, and, subsequently, the female fate is suppressed (Capel, 2017; Swain & Lovell-Badge, 1999; Wilhelm et al., 2007). Distinct gene regulatory networks promote the male or female fate and are regulated by strong feedback loops that antagonize each other, canalizing one fate from the other (Capel, 2017). Sexual fate is interchangeable even after the initial commitment to Sertoli cells or granulosa cells with the removal of specific, critical transcription factors. The loss of *Dmrt1* in Sertoli cells leads to derepression of *Foxl2*, a master regulator of granulosa cell fate, and transdifferentiation of cell fate from Sertoli to granulosa cells (Matson et al., 2011; Matson & Zarkower, 2012). On the other hand, the loss of *Foxl2* in granulosa cells leads to derepression of the male gene network and transdifferentiation of cell fate from granulosa to Sertoli cells (Uhlenhaut et al., 2009). These findings, together with follow-up studies (Li et al., 2017; Lindeman et al., 2015; Minkina et al., 2014; Nicol et al., 2018; Zhao, Svingen, Ng, & Koopman, 2015), suggest that active repression of the alternate sexual fate is important for both testicular and ovarian function, even in adult life.

Epigenetic silencing mechanisms serve as molecular switches for the sex determination of bipotential somatic cell precursors. The deletion of a Polycomb gene *Cbx2* results in male to female

reversal (Katoh-Fukui et al., 1998), which is mediated through suppression of genes required for the female fate (Garcia-Moreno et al., 2019). Additionally, regulation of H3K9 methylation is important for the male sexual fate (Kuroki et al., 2013). Although these studies highlight the importance of epigenetic mechanisms for initial sex determination, the epigenetic mechanisms by which male cellular identity is maintained through cell divisions and the proliferation of Sertoli cells remain to be determined.

Polycomb proteins suppress non-lineage-specific genes and define cellular identities of each lineage in stem cells and in development (Aloia, Di Stefano, & Di Croce, 2013; Ringrose & Paro, 2007; Simon & Kingston, 2013). In this study, we show that Polycomb suppresses the female gene regulatory network in postnatal Sertoli cells, thereby promoting the male gene regulatory network to ensure male cell fate. We generated loss-of-function mouse models of Polycomb repressive complex 1 (PRC1) in Sertoli cells after initial sex determination. We show that PRC1 is required for the proliferation of Sertoli cells, as well as the suppression of non-lineage-specific genes and the female gene regulatory network in Sertoli cells. Taken together, we identify a critical mechanism centered on Polycomb that maintains male fate in adult testes.

Results

PRC1 in Sertoli cells is required for the maintenance of spermatogenesis. In postnatal Sertoli cells (which are detected by the Sertoli cell marker GATA4), RNF2 is highly expressed and the RNF2-mediated epigenetic mark H2AK119ub is abundant (Figure 1A), which suggests PRC1 functions in these cells. To determine the function of PRC1, we generated a PRC1 loss-of-function mouse model by removing two redundant catalytic subunits, RNF2 and RING1 (Endoh et al., 2012). We generated a conditional deletion of *Rnf2* (*Rnf2*cKO) using *Amh*-Cre, which is expressed specifically in Sertoli cells after embryonic day 14.5 (E14.5) (Holdcraft & Braun, 2004), in a background of *Ring1*-knockout (KO) mice (*Amh*-Cre; *Rnf2*cKO; *Ring1*-KO: termed PRC1^{Amh-}

96 ^{Cre}cKO: PRC1AcKO). Although RNF2 appears to be the most active component in the
97 heterodimeric E3 ligases of PRC1, the RNF2 paralog RING1 can partially compensate for the loss
98 of RNF2 (Endoh et al., 2012). Therefore, we made a conditional deletion of *Rnf2* in a background
99 of *Ring1*-KO mice, which are viable and do not have fertility defects (del Mar Lorente et al., 2000).
100 This strategy enabled us to define the function of RNF2 without compensation from RING1, while
101 also representing a "complete" loss-of-function of PRC1 as shown in testicular germ cells
102 (Maezawa et al., 2017) and in other biological contexts (Endoh et al., 2012; Posfai et al., 2012;
103 Yokobayashi et al., 2013). Since PRC1 has various components, including CBX2 (Gao et al., 2012),
104 this strategy allows us to determine the global function of PRC1. At the same time, the use of *Amh*-
105 Cre allowed us to test the function of PRC1, specifically after the completion of sex determination
106 at E12.5.
107
108 PRC1AcKO males have smaller testes compared with littermate controls that harbored
109 floxed alleles for *Rnf2* on a *Ring1*-KO background without *Amh*-Cre (termed PRC1 control:
110 PRC1ctrl: Figure 1B and C). We confirmed efficient *Amh*-Cre-mediated recombination by
111 observing depletion of the RNF2-mediated mark, H2AK119ub, in GATA4^{+} Sertoli cells of
112 PRC1AcKO testes at E15.5 (> 95 % efficiency: Figure 1D) and at postnatal day 7 (P7: Figure 1E).
113 In 6 week-old PRC1AcKO testes, while the tubules with H2AK119ub^{+} Sertoli cells (escaped Cre-
114 mediated deletion) appear to have normal morphology, we frequently observed disorganization of
115 testicular tubules that contain H2AK119ub^{-} Sertoli cells (underwent Cre-mediated deletion:
116 arrowheads, Figure 1- figure supplement 1), suggesting a critical function of PRC1 in Sertoli cells
117 in the organization of testicular tubules. This mosaic pattern is presumably due to incomplete Cre-
118 mediated recombination, as the Sertoli cells that escaped Cre-mediated recombination might have
119 repopulated the testes. Consistent with this interpretation, PRC1AcKO males are subfertile, and 9
120 out of 15 wild-type females mated with 8-11-week old PRC1AcKO males gave birth (Figure 1F)
121 at comparable litter sizes (Figure 1G). Interestingly, fecundity decreased in aged PRC1AcKO males

122 (5 months old), as litter sizes were smaller as compared to controls (Figure 1G). To further examine
123 the phenotype, we measured the blood levels of three hormones critical for testicular homeostasis:
124 although the levels of testosterone and estradiol were comparable between cKO and control mice,
125 follicle-stimulating hormone was increased in mutants (Figure 1H). As follicle stimulating
126 hormone levels are regulated by a feedback mechanism involving Sertoli cells (Oduwole, Peltoketo,
127 & Huhtaniemi, 2018), we infer that the dysfunction of Sertoli cells and testicular degeneration
128 caused increased follicle stimulating hormone levels to recover Sertoli cell function.
129
130 To determine the cause of testicular degeneration, we next examined the proliferation of
131 Sertoli cells. In normal mouse development, Sertoli cells proliferate in fetal and neonatal testes
132 until approximately 2 weeks after birth, and the number of Sertoli cells in adult testes determines
133 both testis size and daily sperm production (Sharpe, McKinnell, Kivlin, & Fisher, 2003). In P7
134 control testes, GATA4^{+} Sertoli cells occasionally co-expressed an S phase marker, PCNA, and
135 another marker of active cell cycle, Ki67 (Figure 2A), consistent with the active proliferation of
136 Sertoli cells. However, in PRC1AcKO testes, GATA4^{+} Sertoli cells were largely devoid of PCNA
137 and Ki67 (Figure 2A), suggesting impaired proliferation of PRC1AcKO Sertoli cells. Next, we
138 independently confirmed the proliferation phenotype by using EdU labeling of actively
139 proliferating cells. EdU was abdominally administrated to P7 mice, and testicular sections were
140 examined the following day. While GATA4^{+} Sertoli cells were occasionally EdU^{+} (approximately
141 one-fouth) in control testes , GATA4^{+} Sertoli cells were devoid of EdU signal in PRC1AcKO testes
142 (Figure 2B). Additional labeling of H2AK119ub confirmed the loss of PRC1 function in GATA4^{+}
143 Sertoli cells from PRC1AcKO testes (Figure 2B). From these results, we conclude that the loss of
144 PRC1 disrupts the proliferation of Sertoli cells. This is in contrast with PRC1's function in testicular
145 germ cells, in which the loss of PRC1 does not affect proliferation but instead causes apoptotic cell
146 death (Maezawa et al., 2017). This difference suggests a unique function of PRC1 in Sertoli cells
147 that is distinct from its function in germ cells.

148

149 **In Sertoli cells, PRC1 suppresses genes required for granulosa cells.** We next sought to
150 determine the genes regulated by PRC1 in Sertoli cells. In PRC1AcKO testes, some Sertoli cells
151 escaped *Amh*-Cre-mediated recombination. Thus, it was difficult to specifically isolate Sertoli cells
152 that underwent PRC1 depletion. To precisely determine the function of PRC1 in gene regulation in
153 Sertoli cells, we used an alternative strategy: we isolated Sertoli cells from a mouse line in which
154 conditional deletion of PRC1 can be induced by tamoxifen-inducible Cre-mediated recombination
155 under the control of the endogenous ROSA26 promoter (*ROSA26*-Cre^{ERT}; *Rnf2*$^{floxed/floxed}$; *Ring1*-
156 KO: termed PRC1$^{ROSA26\text{-}CreERT}$cKO: PRC1RcKO). After isolating Sertoli cells from P7 testes, we
157 cultured Sertoli cells for 4 days in the presence of 4-hydroxytamoxifen (4-OHT), and performed
158 RNA-sequencing (RNA-seq: Figure 3A). As a control, we isolated Sertoli cells from control mice
159 (*Rnf2*$^{floxed/floxed}$; *Ring1*-KO) and cultured them in the same 4-OHT conditions. We performed RNA-
160 seq for two independent biological replicates and confirmed reproducibility between biological
161 replicates (Figure 3- figure supplement 1A).

162

163 Our RNA-seq analyses demonstrated that 338 genes were upregulated in PRC1RcKO
164 Sertoli cells as compared to controls, while 307 genes were downregulated in PRC1RcKO Sertoli
165 cells (Figure 3A and B). Gene ontology (GO) analysis showed that upregulated genes were enriched
166 for functions in neural differentiation, skeletal system, and cell adhesion (Figure 3D). These
167 categories suggest that PRC1 suppressed expression of non-lineage-specific genes in Sertoli cells.
168 On the other hand, GO analysis revealed that downregulated genes were enriched for functions in
169 the cell cycle and M phase (Figure 3D). This result is in accord with the cell cycle arrest we found
170 in PRC1AcKO Sertoli cells (Figure 2).

171

172 Since we anticipated suppression of genes required for granulosa cells by PRC1 in Sertoli
173 cells, we next investigated the expression level of key genes required for granulosa cells. In

174 PRC1RcKO Sertoli cells, genes required for female sexual development were upregulated: these
175 genes included *Rspo1,* an activator of the Wnt pathway (Chassot et al., 2008), and *Foxl2,* a key
176 transcription factor for granulosa cells (Schmidt et al., 2004) (Figure 3E). Importantly, these female
177 genes suppress the male fate, and the loss of these genes leads to female-to-male sex reversal
178 (Ottolenghi et al., 2007; Parma et al., 2006; Schmidt et al., 2004). Consistent with the antagonistic
179 function of these female genes with the male pathway, key sex determination genes for the male
180 pathway were downregulated in PRC1RcKO Sertoli cells: these genes included *Sox9,* an
181 evolutionarily conserved gene for sex determination, which directs the male pathway downstream
182 of *Sry* (Vidal, Chaboissier, de Rooij, & Schedl, 2001), and *Dmrt1* (Raymond, Murphy, O'Sullivan,
183 Bardwell, & Zarkower, 2000; Raymond et al., 1998), male-determining signalling (Figure 3E).
184
185 To determine whether the suppression of female genes was directly regulated by PRC1, we
186 performed chromatin immunoprecipitation sequencing (ChIP-seq) of PRC1-mediated H2AK119ub
187 in isolated wild-type Sertoli cells. We further performed ChIP-seq of H3K27me3 in Sertoli cells
188 since PRC2-mediated H3K27me3 is regulated by PRC1 and its mediated mark H2A119ub
189 (Blackledge et al., 2014; Cooper et al., 2014). We performed ChIP-seq for two independent
190 biological replicates and confirmed the reproducibility between biological replicates (Figure 3-
191 figure supplement 1B). We confirmed the enrichment of H2AK119ub and H3K27me3 around
192 transcription start sites (TSSs) of *Rspo1* and *Foxl2* (Figure 3F). Compared to the enrichment of
193 H2AK119ub on these female genes, enrichment of H2AK119ub was relatively low on the TSSs of
194 the male genes, *Sox9* and *Dmrt1*. Therefore, we conclude that PRC1 directly binds and suppresses
195 *Rspo1* and *Foxl2*.
196
197 Track views of these ChIP-seq data show that all three marks were enriched at *Foxl2* and
198 *Rspo1* loci (Figure 4A). Furthermore, enrichment of these three marks was found in other loci such

199 as *Foxf2*, the mutation of which appears in patients with disorders of sex development (Jochumsen
200 et al., 2008), and *Hoxd13*, which is involved in female reproductive tract development (Du &
201 Taylor, 2015). These results suggest that PRC1 works with PRC2 to suppress female genes as well
202 as developmental regulators such as *Fox* and *Hox* genes, which are the classical targets of
203 Polycomb-mediated gene repression (Lee et al., 2006).
204
205 To determine the features of genome-wide gene repression mediated by Polycomb
206 complexes, we analyzed the enrichment of H2AK119ub, H3K27me3, and RNF2 on the upregulated
207 genes in PRC1RcKO Sertoli cells. H2AK119ub, H3K27me3, and RNF2 were all significantly
208 enriched on the TSSs of upregulated genes in PRC1RcKO Sertoli cells as compared to all genes in
209 the genome (Figure 4B). Additional enrichment analysis confirmed the co-enrichment of
210 H2AK119ub and H3K27me3 (Figure 4C*,* upper panels) as well as co-enrichment of H2AK119ub
211 and RNF2 (Figure 4C*,* lower panels) on upregulated genes in PRC1RcKO Sertoli cells.
212 Furthermore, average tag density analysis confirmed that enrichment of H2AK119ub on
213 upregulated genes in PRC1RcKO Sertoli cells occured on upstream regions, gene bodies, and
214 downstream regions with the highest enrichment near TSSs (Figure 4D). We found a similar
215 distribution of H3K27me3 around the gene bodies of upregulated genes in PRC1RcKO Sertoli cells
216 (Figure 4- figure supplement 1). Together, these results confirmed the genome-wide, global
217 functions of PRC1 in the direct regulation of gene repression in Sertoli cells.
218
219 **Polycomb globally inactivates the female gene regulatory network in postnatal Sertoli cells.**
220 Previous studies have suggested that sex determination is canalized by the interconnected,
221 antagonistic network of genes both in males and in females that are controlled by feedback
222 mechanisms (Capel, 2017). Since Polycomb is implicated in the maintenance of sex-specific gene
223 regulatory networks through the PRC2-mediated mark H3K27me3 (Garcia-Moreno et al., 2019),
224 we hypothesized that PRC1 globally inactivates the female gene regulatory network in postnatal

225 Sertoli cells. Since male- and female-specific gene networks are regulated immediately after sex
226 determination during fetal stages (Jameson et al., 2012), we reasoned that female gene network
227 suppression in fetal Sertoli cells is maintained by PRC1 in postnatal Sertoli cells. To test this
228 hypothesis, we examined the expression profiles of specifically expressed genes in E13.5 granulosa
229 cells (Jameson et al., 2012) (Figure 5- figure supplement 1), termed "pre-granulosa genes" in
230 postnatal Sertoli cells. We found that pre-granulosa genes were upregulated in PRC1RcKO
231 postnatal Sertoli cells as compared to other genes (Figure 5A). On the other hand, specifically
232 expressed genes in E13.5 Sertoli cells (Jameson et al., 2012) (Figure 5- figure supplement 1),
233 termed "pre-Sertoli genes," were downregulated in PRC1RcKO postnatal Sertoli cells as compared
234 to other genes (Figure 5A). We further examined the correlation of each gene and found that pre-
235 granulosa genes were highly correlated with upregulated genes in PRC1RcKO postnatal Sertoli
236 cells, while pre-Sertoli genes were highly correlated with downregulated genes in PRC1RcKO
237 postnatal Sertoli cells (Figure 5B). These results suggest that PRC1 maintains suppression of the
238 female gene regulatory network, which is initiated at the time of sex determination and is
239 maintained throughout the development of postnatal Sertoli cells.
240
241 We next sought to determine whether PRC1 directly suppresses the female gene regulatory
242 network in postnatal Sertoli cells. H2AK119ub is significantly enriched on TSSs of pre-granulosa
243 genes compared to other genes and pre-Sertoli genes (Figure 5C). Among pre-granulosa genes,
244 enrichment of H2AK119ub is positively correlated with upregulated genes in PRC1RcKO
245 postnatal Sertoli cells (Figure 5D). We further identified the enrichment of H3K27me3 on TSSs of
246 pre-granulosa genes in postnatal Sertoli cells (Figure 5- figure supplement 2A), and the correlation
247 between H3K27me3 and upregulated genes on the pre-granulosa genes in PRC1RcKO postnatal
248 Sertoli cells (Figure 5- figure supplement 2B). Together, we conclude that PRC1 globally
249 inactivates the female gene regulatory network in postnatal Sertoli cells.
250

251 **Discussion**

252 In this study, we demonstrated that PRC1 is required for proliferation of Sertoli cells and
253 suppression of the non-lineage-specific gene expression program and the female gene regulatory
254 network. Among these functions, we infer that suppression of the female gene regulatory network
255 is the key mechanism to ensure male fate in addition to canonical functions of PRC1, which controls
256 proliferation and suppression of non-lineage-specific gene expression programs. Although we did
257 not observe complete infertility using *Amh*-Cre, presumably due to the repopulation of Sertoli cells
258 that escaped Cre-mediated recombination, smaller testis size and abnormal tubule organization of
259 cKO testes (Figure 1) suggest that PRC1 is critical for physiological functions of Sertoli cells.
260 Below, we discuss two molecular aspects underlying these physiological phenotypes: control of
261 proliferation and suppression of the female gene regulatory network.

262

263 The proliferation of Sertoli cells is a critical determinant of testicular functions because the
264 number of Sertoli cells defines testicular functions (Sharpe et al., 2003). Rapid proliferation is a
265 prominent feature of juvenile Sertoli cells. In general, Polycomb proteins are associated with the
266 cell cycle checkpoint by directly suppressing the tumor suppressor locus *Cdkn2a*/*Ink4a*/*Arf* (Jacobs,
267 Kieboom, Marino, DePinho, & van Lohuizen, 1999), which functions as a barrier to cancer
268 transformation (Serrano et al., 1996). Therefore, enhanced Polycomb activity is a frequent feature
269 of human tumors. We found that *Cdkn2a* was derepressed in PRC1RcKO Sertoli cells
270 (approximately 2.5-fold upregulation: PRKM value for PRC1RcKO: 32.1 v.s. PRC1ctrl: 13.0).
271 Therefore, our results suggest that PRC1 promotes the rapid proliferation of Sertoli cells by
272 suppressing *Cdkn2a.* The function of PRC1 in Sertoli cell proliferation is distinct from Polycomb
273 functions in testicular germ cells, where PRC1 depletion does not alter the proliferation of germ
274 cells (Maezawa et al., 2017). This may be due to the fact that PRC1 and PRC2 are not required for
275 suppression of *Cdkn2a* in germ cells (Maezawa et al., 2017; Mu, Starmer, Fedoriw, Yee, &
276 Magnuson, 2014). The functional difference in testicular germ cells and Sertoli cells highlights the

277 context-dependent functions of Polycomb proteins. However, a recent study revealed a novel
278 activity by which PcGs can regulate cell proliferation through DNA replication independently of
279 *Cdkn2a* (Piunti et al., 2014). Therefore, determining the detailed molecular mechanisms by which
280 PRC1 controls the proliferation of Sertoli cells will be important for future studies.
281
282 Another critical function of PRC1 in Sertoli cells is the suppression of the female gene
283 regulatory network. DMRT1 is a critical transcription factor that suppresses the expression of
284 female genes (Matson et al., 2011). While more than 10-fold upregulation of the female genes
285 (*Rspo1* and *Foxl2*) was observed for *Dmrt1* mutants (Matson et al., 2011), the degree of
286 upregulation of these genes was modest in PRC1RcKO Sertoli cells (Figure 3). This finding,
287 combined with genetic evidence, indicates that DMRT1 could be the direct regulator of suppression
288 of female genes, while PRC1-mediated mechanisms could be a maintenance mechanism in
289 response to the primary silencing mechanisms determined by DMRT1. Another possibility is
290 compensation by PRC1-independent suppression mechanisms. While a portion of PRC2-mediated
291 H3K27me3 is regulated by variant PRC1 (Blackledge et al., 2014; Cooper et al., 2014), another
292 portion of H3K27me3, mediated by canonical PRC1 and PRC2 complexes, is not downstream of
293 PRC1 (Laugesen, Hojfeldt, & Helin, 2019). These PRC2-mediated mechanisms or other silencing
294 machinery may be responsible for the suppression of female genes.
295
296 The notion that Polycomb regulates the female gene regulatory network has been supported
297 by other recent evidence. In bipotential precursor cells, genes involved in sex determination are
298 marked with bivalent chromatin domains (Garcia-Moreno et al., 2019) that are prevalent in
299 pluripotent stem cells and in germ cells (Bernstein et al., 2006; Hammoud et al., 2009; Lesch,
300 Dokshin, Young, McCarrey, & Page, 2013; Maezawa, Hasegawa, et al., 2018; Maezawa, Yukawa,
301 Alavattam, Barski, & Namekawa, 2018; Sin, Kartashov, Hasegawa, Barski, & Namekawa, 2015).
302 Maintenance of the male fate was explained by the persistence of H3K27me3 on silent female

genes in Sertoli cells (Garcia-Moreno et al., 2019). Consistent with PRC1's function found in the current study, Polycomb-mediated silencing may globally suppress the female gene regulatory network. We found that H2AK119ub was largely associated with this group of female genes (Figure 5). Therefore, it would be interesting to speculate that antagonistic male and female networks can be directly coordinated by Polycomb protein functions, including the strong feedback mechanism underlying both networks. These possibilities raise several outstanding questions to be addressed in future studies. What are the functions of another Polycomb complex, PRC2, and of each Polycomb complex component, including CBX2, in postnatal Sertoli cells? What is the function of Polycomb in female granulosa cells, especially in the suppression of the male gene regulatory network? Does Polycomb underlie the feedback regulation of each network to define sexual identity? Our current study provides a foundation to explore these questions.

Methods

Animals

Generation of mutant *Ring1* and *Rnf2* floxed alleles were previously reported (Cales et al., 2008). *Amh-Cre* transgenic mice were purchased from The Jackson Laboratory (Stock No: 007915) (Holdcraft & Braun, 2004). *Rosa-Cre ERT* mice were purchased from The Jackson Laboratory (Stock No: 008463) (Ventura et al., 2007). A minimum of three independent mice were analyzed for each experiment. All of the animals were handled according to approved institutional animal care and use committee (IACUC) protocols (#IACUC2018-0040) of Cincinnati Children's Hospital Medical Center. Fertility tests were performed with 6-weeks old CD1 female mice (purchased from Charles river). At least 2 female mice were bred with a male mouse for 2 weeks, and the fertility was evaluated by the ratio of pregnant to total female mice and number of pups.

329 **Ligand test**

330 Blood samples were collected from C57BL/6N mice aged 8−11 weeks. Serum was separated
331 immediately and stored at -20°C. Hormone assays, including testosterone, estradiol, and follicle
332 stimulating hormone, were performed by the Center for Research in Reproduction at the University
333 of Virginia.

334

335 **Sertoli cell isolation**

336 Sertoli cells were isolated as previously described with minor modifications (Chang, Lee-Chang,
337 Panneerdoss, MacLean, & Rao, 2011) and collected from C57BL/6N mice aged 6–8 days. Testes
338 were collected in a 24-well plate in Dulbecco's Modified Eagle Medium (DMEM) supplemented
339 with GlutaMax (Thermo Fisher Scientific), non-essential amino acids (NEAA) (Thermo Fisher
340 Scientific), and penicillin and streptomycin (Thermo Fisher Scientific). After removing the *tunica*
341 *albuginea* membrane, testes were digested with collagenase (1 mg/ml) at 34°C for 20 min to
342 remove interstitial cells, then centrifuged at 188×*g* for 5 min. Tubules were washed with medium
343 and then digested with trypsin (2.5 mg/ml) at 34°C for 20 min to obtain a single-cell suspension.
344 To remove KIT-positive spermatogonia, cells were washed with magnetic cell-sorting (MACS)
345 buffer (PBS supplemented with 0.5% BSA and 5 mM EDTA) and incubated with CD117 (KIT)
346 MicroBeads (Miltenyi Biotec) on ice for 20 min. Cells were separated by autoMACS Pro Separator
347 (Miltenyi Biotec) with the program "possel." Cells in the flow-through fraction were washed with
348 MACS buffer and incubated with CD90.2 (THY1) MicroBeads (Miltenyi Biotec) on ice for 20 min
349 to remove THY1-positive spermatogonia. Cells were separated by autoMACS Pro Separator
350 (Miltenyi Biotec) with the program "posseld." Cells in the flow-through fraction were washed and
351 plated in a 6-well plate for 1 h in the medium supplemented with 10% fetal bovine serum, which
352 promotes adhesion of Sertoli cells. Purity was confirmed by immunostaining.

353 For PRC1RcKO, cells were cultured for 4 days with 1 μM 4-OHT in Dulbecco's Modified
354 Eagle Medium (DMEM) supplemented with GlutaMax (Thermo Fisher Scientific), non-essential
355 amino acids (NEAA) (Thermo Fisher Scientific), and penicillin and streptomycin (Thermo Fisher
356 Scientific). The same medium was replaced 2 days after the initiation of the culture.
357

358 **Histological analysis and germ cell slide preparation**

359 For the preparation of testicular paraffin blocks, testes were fixed with 4% paraformaldehyde (PFA)
360 overnight at 4°C with gentle inverting. Testes were dehydrated and embedded in paraffin. For
361 histological analysis, 7 μm-thick paraffin sections were deparaffinized and stained with
362 hematoxylin and eosin. For immunofluorescence analysis of testicular sections, antigen retrieval
363 was performed by boiling the slides in target retrieval solution (DAKO) for 10 min and letting the
364 solution cool for 30 min. Sections were blocked with Blocking One Histo (Nacalai) for 1 h at room
365 temperature and then incubated with primary antibodies overnight at 4°C. The resulting signals
366 were detected by incubation with secondary antibodies conjugated to fluorophores (Thermo Fisher
367 Scientific). Sections were counterstained with DAPI. Images were obtained via a laser scanning
368 confocal microscope A1R (Nikon) and processed with NIS-Elements (Nikon) and ImageJ
369 (National Institutes of Health) (Schneider, Rasband, & Eliceiri, 2012).
370

371 **ChIP-sequencing, RNA-sequencing, and data analysis**

372 RNA-seq analyses were performed in the BioWardrobe Experiment Management System
373 (Kartashov & Barski, 2015). Briefly, reads were aligned by STAR (version STAR_2.5.3a) with
374 default arguments except --outFilterMultimapNmax 1 and --outFilterMismatchNmax 2. The --
375 outFilterMultimapNmax parameter was used to allow unique alignments only, and the --
376 outFilterMismatchNmax parameter was used to allow a maximum of 2 errors. NCBI RefSeq
377 annotation from the mm10 UCSC genome browser was used, and canonical TSSs (1 TSS per gene)
378 were analyzed. All reads from the resulting .bam files were split for related isoforms with respect

379 to RefSeq annotation. Then, the EM algorithm was used to estimate the number of reads for each
380 isoform. To detect differentially expressed genes between two biological samples, a read count
381 output file was input to the DESeq2 package (version 1.16.1); then, the program functions
382 DESeqDataSetFromMatrix and DESeq were used to compare each gene's expression level between
383 two biological samples. Differentially expressed genes were identified through binominal tests,
384 thresholding Benjamini-Hochberg- adjusted P values to <0.01. To perform gene ontology analyses,
385 the functional annotation clustering tool in DAVID (version 6.8) was used, and a background of all
386 mouse genes was applied. Biological process term groups with a significance of $P < 0.05$ (modified
387 Fisher's exact test) were considered significant.

388 Cross-linking ChIP-seq with the ChIPmetation method (Schmidl, Rendeiro, Sheffield, &
389 Bock, 2015) was performed for H2AK119ub, H3K27me3, and RNF2 as described previously
390 (Schmidl et al., 2015). Data analysis for both ChIP-seq and RNA-seq was performed in the
391 BioWardrobe Experiment Management System (https://github.com/Barski-lab/biowardrobe
392 (Kartashov & Barski, 2015)). Briefly, reads were aligned to the mouse genome (mm10) with
393 Bowtie (version 1.0.0 (Langmead, Trapnell, Pop, & Salzberg, 2009)), assigned to RefSeq genes
394 (which have one annotation per gene) using the BioWardrobe algorithm, and displayed on a local
395 mirror of the UCSC genome browser as coverage. Peaks of H2AK119ub-, H3K27me3- and RNF2-
396 enrichment were identified using MACS2 (version 2.0.10.20130712 (Zhang et al., 2008)). Pearson
397 correlations for the genome-wide enrichment of the peaks among ChIP-seq library replicates were
398 analyzed using SeqMonk (Babraham Institute). Average tag density profiles were calculated
399 around gene bodies, including 5-kb upstream and 5-kb downstream of the genes. Resulting graphs
400 were smoothed in 200-bp windows. Enrichment levels for ChIP-seq experiments were calculated
401 for 4-kb windows, promoter regions of genes (±2 kb surrounding TSSs), and enhancer regions. To
402 normalize tag value read counts were multiplied by 1,000,000 and then divided by the total number
403 of reads in each nucleotide position. The total amount of tag values in promoter or enhancer regions
404 were calculated as enrichment. Microarray data was analyzed using the processed data (Jameson

et al., 2012). Differentially expressed genes were identified through a p-value cutoff of 0.05, and a fold change cutoff of 2 for the comparison between E13.5 XX supporting cells and E13.5 XY supporting cells. Highly expressed genes in E13.5 XY supporting cells and in E13.5 XX supporting cells were termed as "Pre-sertoli genes" and "Pre-granulosa genes", respectively. RNA-seq and ChIP-seq data reported in this paper have been deposited in GEO under accession code GSE167516.

Acknowledgments

We thank David Zarkower and Vivian Bardwell for their help and discussion in the initial phase of this project, Katie Gerhardt for editing the manuscript, and the members of the Namekawa and Maezawa laboratories for discussion and helpful comments regarding the manuscript. This work was supported by Japan Society for the Promotion of Science Grant-in-Aid for Research Activity Start-up (19K21196), the Takeda Science Foundation (2019), and the Uehara Memorial Foundation Research Incentive Grant (2018) to SM, NIH Grants DP2GM119134 to AB, R35GM119458 to TD, and R01GM098605 and R01GM122776 to SHN.

Competing Interests

The authors declare no competing interests.

422 **References**

423 Aloia, L., Di Stefano, B., & Di Croce, L. (2013). Polycomb complexes in stem cells and embryonic
424 development. *Development, 140*(12), 2525-2534. doi:10.1242/dev.091553

425 Bernstein, B. E., Mikkelsen, T. S., Xie, X., Kamal, M., Huebert, D. J., Cuff, J., . . . Lander, E. S.
426 (2006). A bivalent chromatin structure marks key developmental genes in embryonic stem
427 cells. *Cell, 125*(2), 315-326. doi:10.1016/j.cell.2006.02.041

428 Blackledge, N. P., Farcas, A. M., Kondo, T., King, H. W., McGouran, J. F., Hanssen, L. L., . . .
429 Klose, R. J. (2014). Variant PRC1 complex-dependent H2A ubiquitylation drives PRC2
430 recruitment and polycomb domain formation. *Cell, 157*(6), 1445-1459.
431 doi:10.1016/j.cell.2014.05.004

432 Cales, C., Roman-Trufero, M., Pavon, L., Serrano, I., Melgar, T., Endoh, M., . . . Vidal, M. (2008).
433 Inactivation of the polycomb group protein Ring1B unveils an antiproliferative role in
434 hematopoietic cell expansion and cooperation with tumorigenesis associated with Ink4a
435 deletion. *Mol Cell Biol, 28*(3), 1018-1028. doi:10.1128/MCB.01136-07

436 Capel, B. (2017). Vertebrate sex determination: evolutionary plasticity of a fundamental switch.
437 *Nat Rev Genet, 18*(11), 675-689. doi:10.1038/nrg.2017.60

438 Chang, Y. F., Lee-Chang, J. S., Panneerdoss, S., MacLean, J. A., 2nd, & Rao, M. K. (2011). Isolation
439 of Sertoli, Leydig, and spermatogenic cells from the mouse testis. *Biotechniques, 51*(5),
440 341-342, 344. doi:10.2144/000113764

441 Chassot, A. A., Ranc, F., Gregoire, E. P., Roepers-Gajadien, H. L., Taketo, M. M., Camerino, G.,
442 Chaboissier, M. C. (2008). Activation of beta-catenin signaling by Rspo1 controls
443 differentiation of the mammalian ovary. *Human Molecular Genetics, 17*(9), 1264-1277.
444 doi:10.1093/hmg/ddn016

445 Cooper, S., Dienstbier, M., Hassan, R., Schermelleh, L., Sharif, J., Blackledge, N. P., . . .
446 Brockdorff, N. (2014). Targeting polycomb to pericentric heterochromatin in embryonic

447 stem cells reveals a role for H2AK119u1 in PRC2 recruitment. *Cell Rep, 7*(5), 1456-1470.
448 doi:10.1016/j.celrep.2014.04.012
449 del Mar Lorente, M., Marcos-Gutierrez, C., Perez, C., Schoorlemmer, J., Ramirez, A., Magin, T.,
450 & Vidal, M. (2000). Loss- and gain-of-function mutations show a polycomb group function
451 for Ring1A in mice. *Development, 127*(23), 5093-5100.
452 Du, H., & Taylor, H. S. (2015). The Role of Hox Genes in Female Reproductive Tract Development,
453 Adult Function, and Fertility. *Cold Spring Harb Perspect Med, 6*(1), a023002.
454 doi:10.1101/cshperspect.a023002
455 Endoh, M., Endo, T. A., Endoh, T., Isono, K., Sharif, J., Ohara, O., . . . Koseki, H. (2012). Histone
456 H2A mono-ubiquitination is a crucial step to mediate PRC1-dependent repression of
457 developmental genes to maintain ES cell identity. *PLoS Genet, 8*(7), e1002774.
458 doi:10.1371/journal.pgen.1002774
459 Gao, Z., Zhang, J., Bonasio, R., Strino, F., Sawai, A., Parisi, F., . . . Reinberg, D. (2012). PCGF
460 homologs, CBX proteins, and RYBP define functionally distinct PRC1 family complexes.
461 *Mol Cell, 45*(3), 344-356. doi:10.1016/j.molcel.2012.01.002
462 Garcia-Moreno, S. A., Lin, Y. T., Futtner, C. R., Salamone, I. M., Capel, B., & Maatouk, D. M.
463 (2019). CBX2 is required to stabilize the testis pathway by repressing Wnt signaling. *PLoS*
464 *Genet, 15*(5), e1007895. doi:10.1371/journal.pgen.1007895
465 Hammoud, S. S., Nix, D. A., Zhang, H., Purwar, J., Carrell, D. T., & Cairns, B. R. (2009).
466 Distinctive chromatin in human sperm packages genes for embryo development. *Nature,*
467 *460*(7254), 473-478. doi:10.1038/nature08162
468 Holdcraft, R. W., & Braun, R. E. (2004). Androgen receptor function is required in Sertoli cells for
469 the terminal differentiation of haploid spermatids. *Development, 131*(2), 459-467.
470 doi:10.1242/dev.00957

471 Jacobs, J. J., Kieboom, K., Marino, S., DePinho, R. A., & van Lohuizen, M. (1999). The oncogene
472 and Polycomb-group gene bmi-1 regulates cell proliferation and senescence through the
473 ink4a locus. *Nature, 397*(6715), 164-168. doi:10.1038/16476
474 Jameson, S. A., Natarajan, A., Cool, J., DeFalco, T., Maatouk, D. M., Mork, L., . . . Capel, B.
475 (2012). Temporal transcriptional profiling of somatic and germ cells reveals biased lineage
476 priming of sexual fate in the fetal mouse gonad. *PLoS Genet, 8*(3), e1002575.
477 doi:10.1371/journal.pgen.1002575
478 Jochumsen, U., Werner, R., Miura, N., Richter-Unruh, A., Hiort, O., & Holterhus, P. M. (2008).
479 Mutation analysis of FOXF2 in patients with disorders of sex development (DSD) in
480 combination with cleft palate. *Sex Dev, 2*(6), 302-308. doi:10.1159/000195679
481 Kartashov, A. V., & Barski, A. (2015). BioWardrobe: an integrated platform for analysis of
482 epigenomics and transcriptomics data. *Genome Biol, 16*, 158. doi:10.1186/s13059-015-
483 0720-3
484 Katoh-Fukui, Y., Tsuchiya, R., Shiroishi, T., Nakahara, Y., Hashimoto, N., Noguchi, K., &
485 Higashinakagawa, T. (1998). Male-to-female sex reversal in M33 mutant mice. *Nature,*
486 *393*(6686), 688-692. doi:10.1038/31482
487 Kuroki, S., Matoba, S., Akiyoshi, M., Matsumura, Y., Miyachi, H., Mise, N., . . . Tachibana, M.
488 (2013). Epigenetic regulation of mouse sex determination by the histone demethylase
489 Jmjd1a. *Science, 341*(6150), 1106-1109. doi:10.1126/science.1239864
490 Langmead, B., Trapnell, C., Pop, M., & Salzberg, S. L. (2009). Ultrafast and memory-efficient
491 alignment of short DNA sequences to the human genome. *Genome Biol, 10*(3), R25.
492 doi:10.1186/gb-2009-10-3-r25
493 Laugesen, A., Hojfeldt, J. W., & Helin, K. (2019). Molecular Mechanisms Directing PRC2
494 Recruitment and H3K27 Methylation. *Mol Cell, 74*(1), 8-18.
495 doi:10.1016/j.molcel.2019.03.011

496 Lee, T. I., Jenner, R. G., Boyer, L. A., Guenther, M. G., Levine, S. S., Kumar, R. M., . . . Young, R.
497 A. (2006). Control of developmental regulators by Polycomb in human embryonic stem
498 cells. *Cell, 125*(2), 301-313. doi:10.1016/j.cell.2006.02.043
499 Lesch, B. J., Dokshin, G. A., Young, R. A., McCarrey, J. R., & Page, D. C. (2013). A set of genes
500 critical to development is epigenetically poised in mouse germ cells from fetal stages
501 through completion of meiosis. *Proc Natl Acad Sci U S A, 110*(40), 16061-16066.
502 doi:10.1073/pnas.1315204110
503 Li, Y., Zhang, L., Hu, Y., Chen, M., Han, F., Qin, Y., . . . Gao, F. (2017). beta-Catenin directs the
504 transformation of testis Sertoli cells to ovarian granulosa-like cells by inducing Foxl2
505 expression. *J Biol Chem, 292*(43), 17577-17586. doi:10.1074/jbc.M117.811349
506 Lindeman, R. E., Gearhart, M. D., Minkina, A., Krentz, A. D., Bardwell, V. J., & Zarkower, D.
507 (2015). Sexual cell-fate reprogramming in the ovary by DMRT1. *Current Biology, 25*(6),
508 764-771. doi:10.1016/j.cub.2015.01.034
509 Maezawa, S., Hasegawa, K., Yukawa, M., Kubo, N., Sakashita, A., Alavattam, K. G., . . .
510 Namekawa, S. H. (2018). Polycomb protein SCML2 facilitates H3K27me3 to establish
511 bivalent domains in the male germline. *Proc Natl Acad Sci U S A, 115*(19), 4957-4962.
512 doi:10.1073/pnas.1804512115
513 Maezawa, S., Hasegawa, K., Yukawa, M., Sakashita, A., Alavattam, K. G., Andreassen, P. R., . . .
514 Namekawa, S. H. (2017). Polycomb directs timely activation of germline genes in
515 spermatogenesis. *Genes Dev, 31*(16), 1693-1703. doi:10.1101/gad.302000.117
516 Maezawa, S., Yukawa, M., Alavattam, K. G., Barski, A., & Namekawa, S. H. (2018). Dynamic
517 reorganization of open chromatin underlies diverse transcriptomes during spermatogenesis.
518 *Nucleic Acids Res, 46*(2), 593-608. doi:10.1093/nar/gkx1052
519 Matson, C. K., Murphy, M. W., Sarver, A. L., Griswold, M. D., Bardwell, V. J., & Zarkower, D.
520 (2011). DMRT1 prevents female reprogramming in the postnatal mammalian testis.
521 *Nature, 476*(7358), 101-104. doi:10.1038/nature10239

522 Matson, C. K., & Zarkower, D. (2012). Sex and the singular DM domain: insights into sexual
523 regulation, evolution and plasticity. *Nat Rev Genet, 13*(3), 163-174. doi:10.1038/nrg3161
524 Minkina, A., Matson, C. K., Lindeman, R. E., Ghyselinck, N. B., Bardwell, V. J., & Zarkower, D.
525 (2014). DMRT1 protects male gonadal cells from retinoid-dependent sexual
526 transdifferentiation. *Dev Cell, 29*(5), 511-520. doi:10.1016/j.devcel.2014.04.017
527 Mu, W., Starmer, J., Fedoriw, A. M., Yee, D., & Magnuson, T. (2014). Repression of the soma-
528 specific transcriptome by Polycomb-repressive complex 2 promotes male germ cell
529 development. *Genes Dev, 28*(18), 2056-2069. doi:10.1101/gad.246124.114
530 Nicol, B., Grimm, S. A., Gruzdev, A., Scott, G. J., Ray, M. K., & Yao, H. H. (2018). Genome-wide
531 identification of FOXL2 binding and characterization of FOXL2 feminizing action in the
532 fetal gonads. *Human Molecular Genetics, 27*(24), 4273-4287. doi:10.1093/hmg/ddy312
533 Oduwole, O. O., Peltoketo, H., & Huhtaniemi, I. T. (2018). Role of Follicle-Stimulating Hormone
534 in Spermatogenesis. *Front Endocrinol (Lausanne), 9*, 763. doi:10.3389/fendo.2018.00763
535 Ottolenghi, C., Pelosi, E., Tran, J., Colombino, M., Douglass, E., Nedorezov, T., . . . Schlessinger,
536 D. (2007). Loss of Wnt4 and Foxl2 leads to female-to-male sex reversal extending to germ
537 cells. *Hum Mol Genet, 16*(23), 2795-2804. doi:10.1093/hmg/ddm235
538 Parma, P., Radi, O., Vidal, V., Chaboissier, M. C., Dellambra, E., Valentini, S., . . . Camerino, G.
539 (2006). R-spondin1 is essential in sex determination, skin differentiation and malignancy.
540 *Nat Genet, 38*(11), 1304-1309. doi:10.1038/ng1907
541 Piunti, A., Rossi, A., Cerutti, A., Albert, M., Jammula, S., Scelfo, A., . . . Pasini, D. (2014).
542 Polycomb proteins control proliferation and transformation independently of cell cycle
543 checkpoints by regulating DNA replication. *Nat Commun, 5*, 3649.
544 doi:10.1038/ncomms4649
545 Posfai, E., Kunzmann, R., Brochard, V., Salvaing, J., Cabuy, E., Roloff, T. C., . . . Peters, A. H.
546 (2012). Polycomb function during oogenesis is required for mouse embryonic
547 development. *Genes Dev, 26*(9), 920-932. doi:10.1101/gad.188094.112

548 Raymond, C. S., Murphy, M. W., O'Sullivan, M. G., Bardwell, V. J., & Zarkower, D. (2000). Dmrt1,
549 a gene related to worm and fly sexual regulators, is required for mammalian testis
550 differentiation. *Genes Dev, 14*(20), 2587-2595. doi:10.1101/gad.834100
551 Raymond, C. S., Shamu, C. E., Shen, M. M., Seifert, K. J., Hirsch, B., Hodgkin, J., & Zarkower,
552 D. (1998). Evidence for evolutionary conservation of sex-determining genes. *Nature,*
553 *391*(6668), 691-695. doi:10.1038/35618
554 Ringrose, L., & Paro, R. (2007). Polycomb/Trithorax response elements and epigenetic memory of
555 cell identity. *Development, 134*(2), 223-232. doi:10.1242/dev.02723
556 Schmidl, C., Rendeiro, A. F., Sheffield, N. C., & Bock, C. (2015). ChIPmentation: fast, robust, low-
557 input ChIP-seq for histones and transcription factors. *Nat Methods, 12*(10), 963-965.
558 doi:10.1038/nmeth.3542
559 Schmidt, D., Ovitt, C. E., Anlag, K., Fehsenfeld, S., Gredsted, L., Treier, A. C., & Treier, M. (2004).
560 The murine winged-helix transcription factor Foxl2 is required for granulosa cell
561 differentiation and ovary maintenance. *Development, 131*(4), 933-942.
562 doi:10.1242/dev.00969
563 Schneider, C. A., Rasband, W. S., & Eliceiri, K. W. (2012). NIH Image to ImageJ: 25 years of image
564 analysis. *Nat Methods, 9*(7), 671-675. Retrieved from
565 https://www.ncbi.nlm.nih.gov/pubmed/22930834
566 Serrano, M., Lee, H., Chin, L., Cordon-Cardo, C., Beach, D., & DePinho, R. A. (1996). Role of the
567 INK4a locus in tumor suppression and cell mortality. *Cell, 85*(1), 27-37.
568 doi:10.1016/s0092-8674(00)81079-x
569 Sharpe, R. M., McKinnell, C., Kivlin, C., & Fisher, J. S. (2003). Proliferation and functional
570 maturation of Sertoli cells, and their relevance to disorders of testis function in adulthood.
571 *Reproduction, 125*(6), 769-784.

572 Simon, J. A., & Kingston, R. E. (2013). Occupying chromatin: Polycomb mechanisms for getting
573 to genomic targets, stopping transcriptional traffic, and staying put. *Mol Cell, 49*(5), 808-
574 824. doi:10.1016/j.molcel.2013.02.013
575 Sin, H. S., Kartashov, A. V., Hasegawa, K., Barski, A., & Namekawa, S. H. (2015). Poised
576 chromatin and bivalent domains facilitate the mitosis-to-meiosis transition in the male
577 germline. *BMC Biol, 13*, 53. doi:10.1186/s12915-015-0159-8
578 Svingen, T., & Koopman, P. (2013). Building the mammalian testis: origins, differentiation, and
579 assembly of the component cell populations. *Genes Dev, 27*(22), 2409-2426.
580 doi:10.1101/gad.228080.113
581 Swain, A., & Lovell-Badge, R. (1999). Mammalian sex determination: a molecular drama. *Genes*
582 *Dev, 13*(7), 755-767. doi:10.1101/gad.13.7.755
583 Uhlenhaut, N. H., Jakob, S., Anlag, K., Eisenberger, T., Sekido, R., Kress, J., . . . Treier, M. (2009).
584 Somatic sex reprogramming of adult ovaries to testes by FOXL2 ablation. *Cell, 139*(6),
585 1130-1142. doi:10.1016/j.cell.2009.11.021
586 Ventura, A., Kirsch, D. G., McLaughlin, M. E., Tuveson, D. A., Grimm, J., Lintault, L., . . . Jacks,
587 T. (2007). Restoration of p53 function leads to tumour regression in vivo. *Nature,*
588 *445*(7128), 661-665. doi:10.1038/nature05541
589 Vidal, V. P., Chaboissier, M. C., de Rooij, D. G., & Schedl, A. (2001). Sox9 induces testis
590 development in XX transgenic mice. *Nat Genet, 28*(3), 216-217. doi:10.1038/90046
591 Wilhelm, D., Palmer, S., & Koopman, P. (2007). Sex determination and gonadal development in
592 mammals. *Physiol Rev, 87*(1), 1-28. doi:10.1152/physrev.00009.2006
593 Yokobayashi, S., Liang, C. Y., Kohler, H., Nestorov, P., Liu, Z., Vidal, M., . . . Peters, A. H. (2013).
594 PRC1 coordinates timing of sexual differentiation of female primordial germ cells. *Nature,*
595 *495*(7440), 236-240. doi:10.1038/nature11918

596 Zhang, Y., Liu, T., Meyer, C. A., Eeckhoute, J., Johnson, D. S., Bernstein, B. E., . . . Liu, X. S.
597 (2008). Model-based analysis of ChIP-Seq (MACS). *Genome Biol, 9*(9), R137.
598 doi:10.1186/gb-2008-9-9-r137
599 Zhao, L., Svingen, T., Ng, E. T., & Koopman, P. (2015). Female-to-male sex reversal in mice caused
600 by transgenic overexpression of Dmrt1. *Development, 142*(6), 1083-1088.
601 doi:10.1242/dev.122184
602

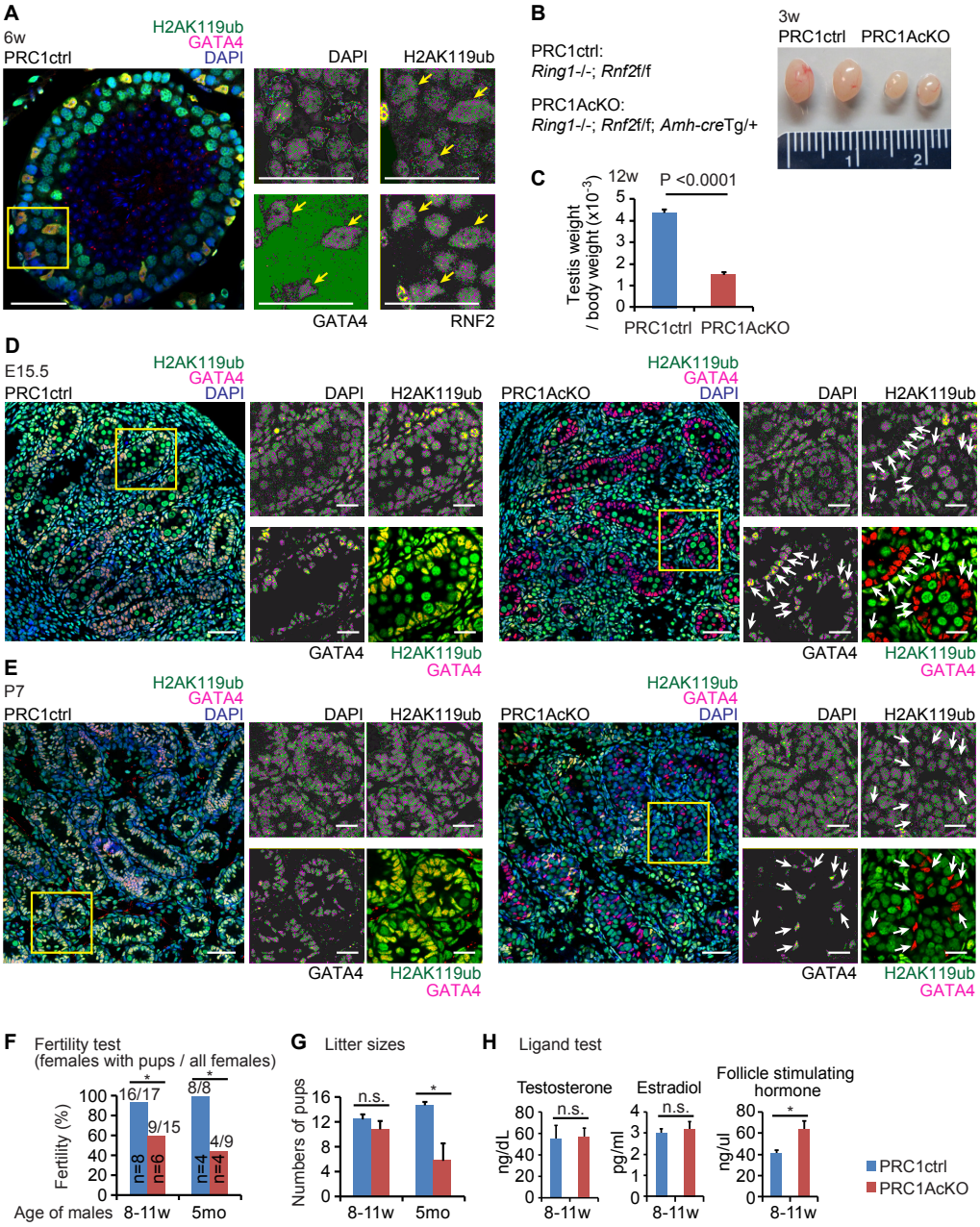

Figure 1. Deletion of PRC1 in Sertoli cells.
(**A**) RNF2 and RNF2-mediated H2AK119ub localized at GATA4-positive Sertoli cells (yellow arrows) in a testicular section at 6 weeks of age. Regions bordered by yellow squares are magnified in the right panels. Bars in the large panels: 50 µm. Bars in the magnified panels: 20 µm. (**B**) Genotypes and photographs of testes at 3 weeks of age. Measurement scale in the panel: 2 cm. (**C**) Testicular weight/body weight ratio ($\times 10^{-3}$) at 12 weeks of age. $P < 0.0001$, unpaired t-test. (**D, E**) Localization of H2AK119ub and GATA4 in PRC1ctrl and PRC1AcKO at embryonic day 15.5 (**D**) and 1 week of age (**E**). Regions bordered by yellow squares are magnified in the right panels. Bars in the large panels: 50 µm. Bars in the magnified panels: 20 µm. H2AK119ub$^-$ Sertoli cells in mutants are shown with white arrows. (**F**) The fertility of PRC1AcKO males, at 8-11 weeks of age and 5 months of age, were tested via crosses with CD1 wild-type females. Numbers of males tested are shown within the bars, and numbers of females with pups and all females are shown above the bars. *$P < 0.05$, Fisher's exact test. (**G**) Litter sizes of breeding tests at 8-11 weeks of age and 5 months of age. *$P < 0.05$, Welch's t-test. (**H**) Ligand hormone tests at 8-11 weeks of age testes. *$P < 0.05$, Welch's t-test. n.s., not significant.

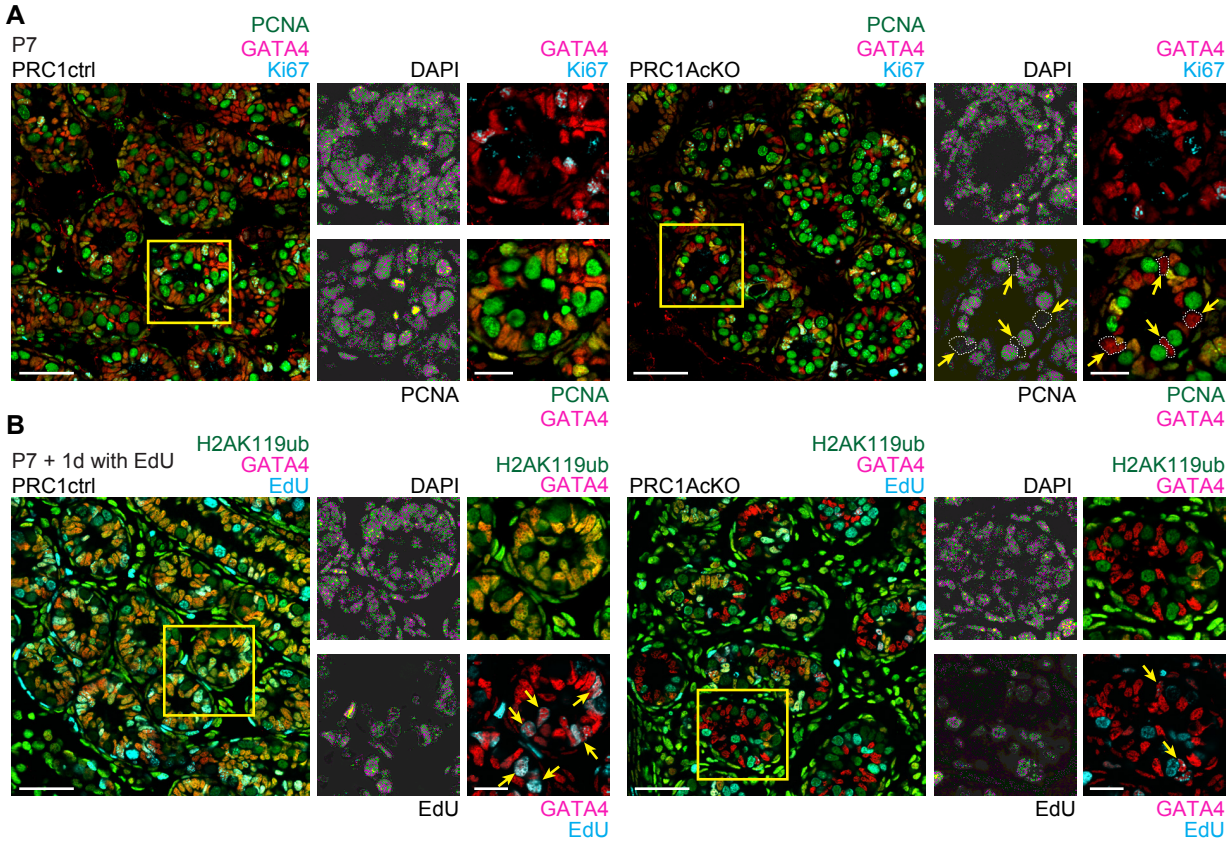

Figure 2. PRC1 is required for proliferation of Sertoli cells.
(**A**) PCNA and Ki67 were not detected in GATA4-positive Sertoli cells (arrows) in a PRC1AcKO testicular section at 6 weeks of age, while PCNA and Ki67 were present in PRC1ctrl Sertoli cells. (**B**) Testicular sections of the indicated genotypes 1 day following the injection of EdU into males at 1 week of age. The presence of EdU-positive Sertoli cells (arrows) was decreased in PRC1AcKO testes. Regions bordered by yellow squares are magnified in the right panels. Bars in the large panels: 50 µm. Bars in the magnified panels: 20 µm.

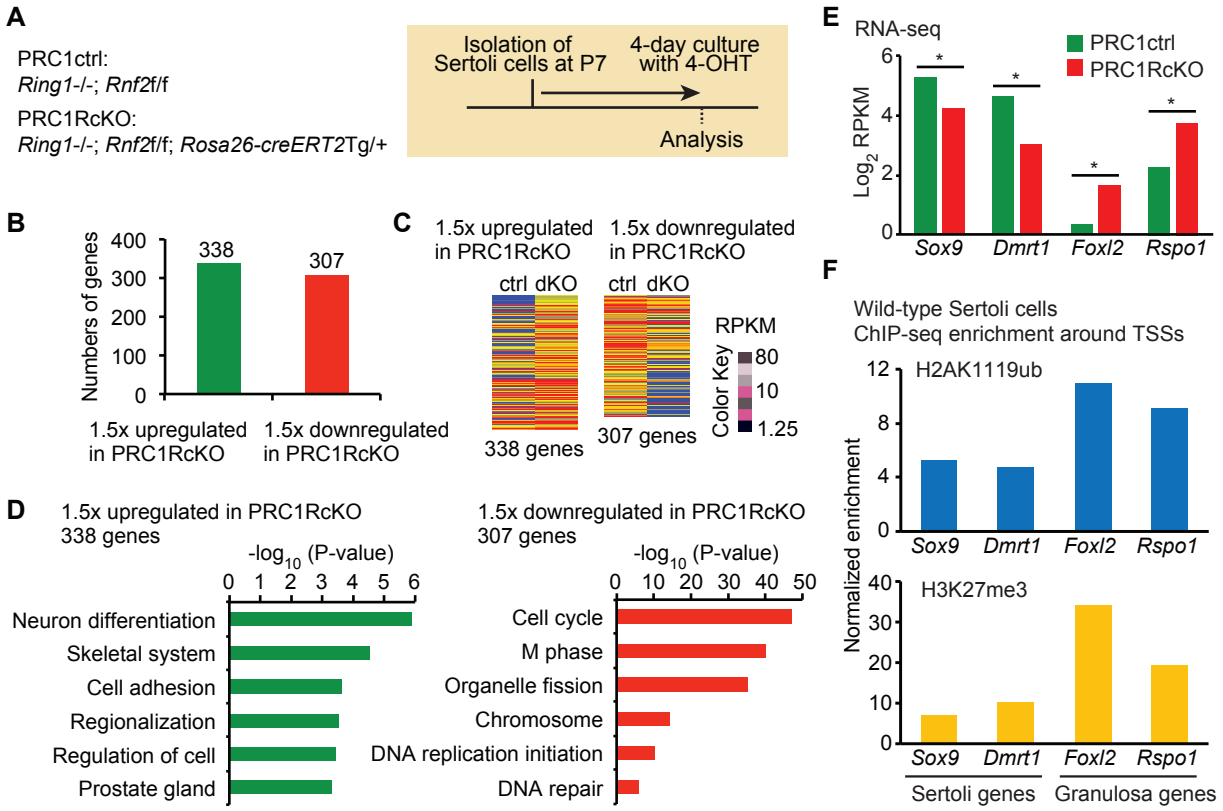

Figure 3. In Sertoli cells, PRC1 suppresses genes required for granulosa cells.
(**A**) Genotypes and experiment schematic. Sertoli cells were isolated from P7 testes and cultured for 4 days in the presence of 4-OHT prior to RNA-seq analyses. (**B**) The numbers of differentially expressed genes detected by RNA-seq (≥1.5-fold change, $P_{adj} < 0.05$) in Sertoli cells (Two biological replicates) between PRC1ctrl and PRC1RcKO. (**C**) Heatmaps showing gene expression patterns for upregulated (left) and down-regulated (right) genes in Sertoli cells. (**D**) GO term analyses. (**E**) Expression levels for representative Sertoli and granulosa genes. (**F, G**) H2AK119ub and H3K27me3 ChIP-seq enrichment around the TSSs of representative Sertoli and granulosa genes.

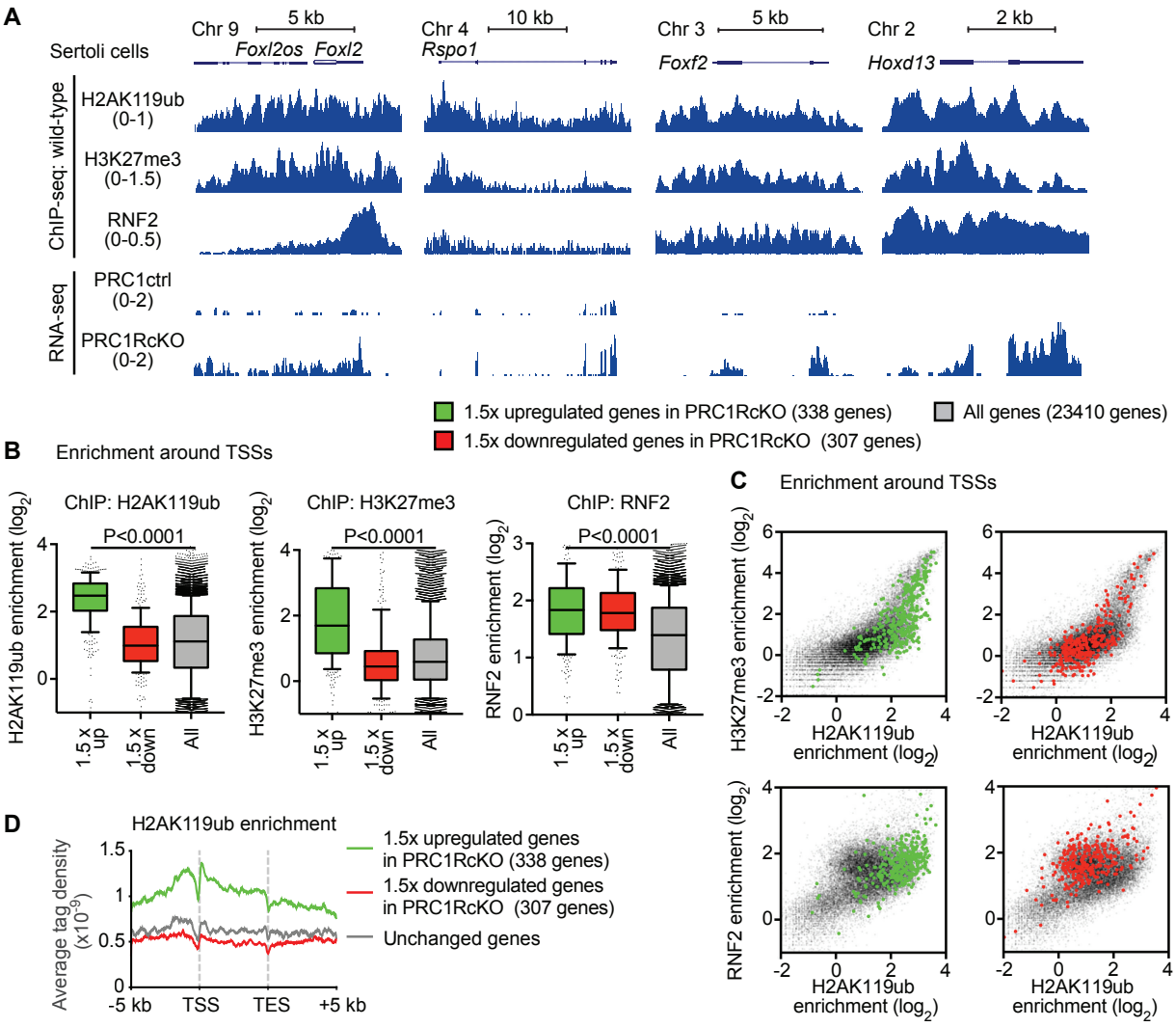

Figure 4. In Sertoli cells, Polycomb-mediated marks are enriched on genes required for granulosa cells. (**A**) Genome track views of representative genes in the female gene regulatory network. ChIP-seq enrichment in wild-type Sertoli cells is shown (top); RNA-seq peaks in PRC1ctrl and PRC1RcKO Sertoli cells are shown (bottom). (**B**) Box-and-whisker plots showing distributions of enrichment for ChIP-seq data. Central bars represent medians, the boxes encompass 50% of the data points, and the whiskers indicate 90% of the data points. *P*, Mann-Whitney U tests. (**C**) Scatter plots showing ChIP-seq enrichment (±2 kb around TSSs) of indicated modifications on genes upregulated (left panels) and down-regulated (right panels) in Sertoli cells. The distribution of all genes is shown with gray dots. (**D**) Average tag densities of H2AK119ub ChIP-seq enrichment.

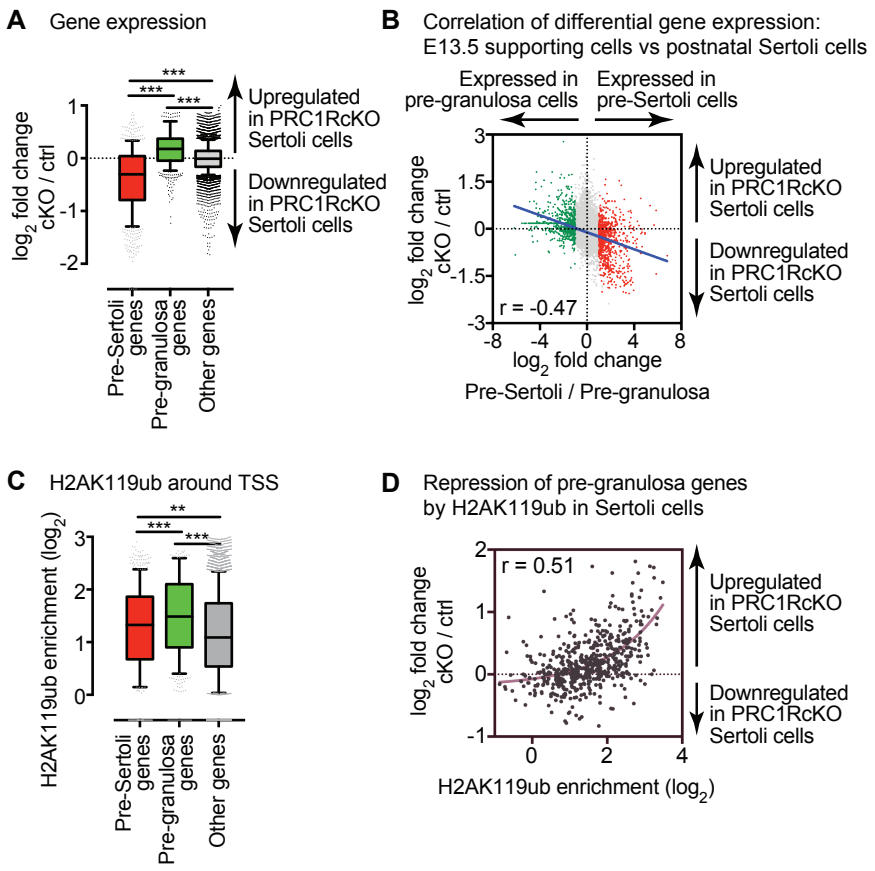

Figure 5. Polycomb inactivates the female gene regulatory network in Sertoli cells.
(**A**) Box-and-whisker plots showing distributions of RNA-seq data. Central bars represent medians, the boxes encompass 50% of the data points, and the whiskers indicate 90% of the data points. *** $P < 0.0001$, Mann-Whitney U tests. (**B**) Scatter plots showing the Pearson correlation between RNA-seq data for genes regulated in E13.5 support cells and P7 Sertoli cells. A linear trendline is shown in blue. (**C**) Box-and-whisker plots showing distributions of enrichment for H2AK119ub ChIP-seq data. Central bars represent medians, the boxes encompass 50% of the data points, and the whiskers indicate 90% of the data points. *** $P < 0.0001$, ** $P < 0.005$, Mann-Whitney U tests. (**D**) Scatter plots showing the Pearson correlation between ChIP-seq enrichment (±2 kb around TSSs) and gene expression in Sertoli cells. A linear trendline is shown in blue.

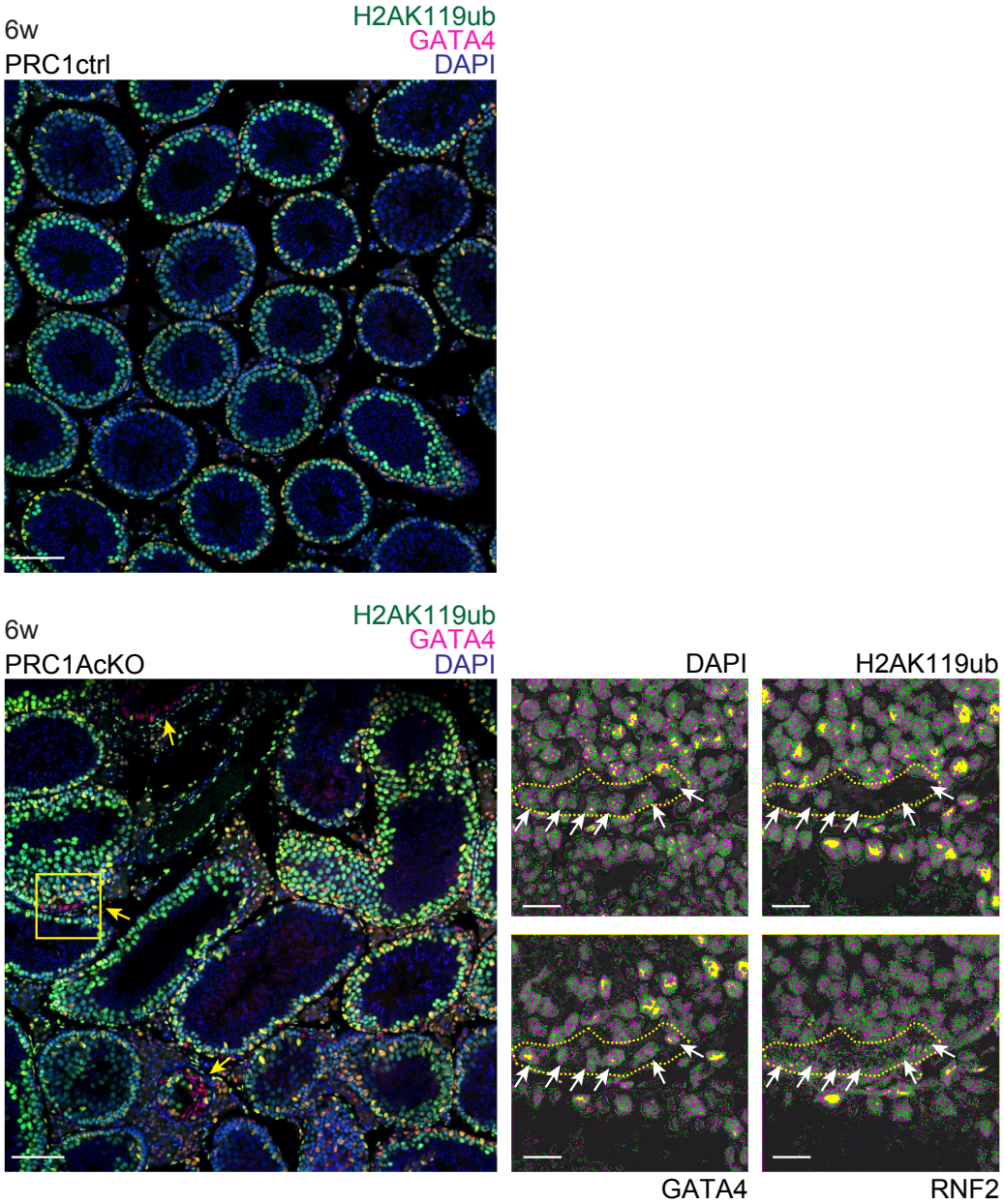

Figure 1- figure supplement 1. Deletion of PRC1 in Sertoli cells causes degeneration of testes at 6 weeks of age. Localization of H2AK119ub and GATA4 in PRC1ctrl and PRC1AcKO at 6 weeks of age. Regions bordered by yellow squares are magnified in the right panels. Bars in the large panels: 50 µm. Bars in the magnified panels: 20 µm. H2AK119ub^{-} Sertoli cells in mutants are shown with white arrows.

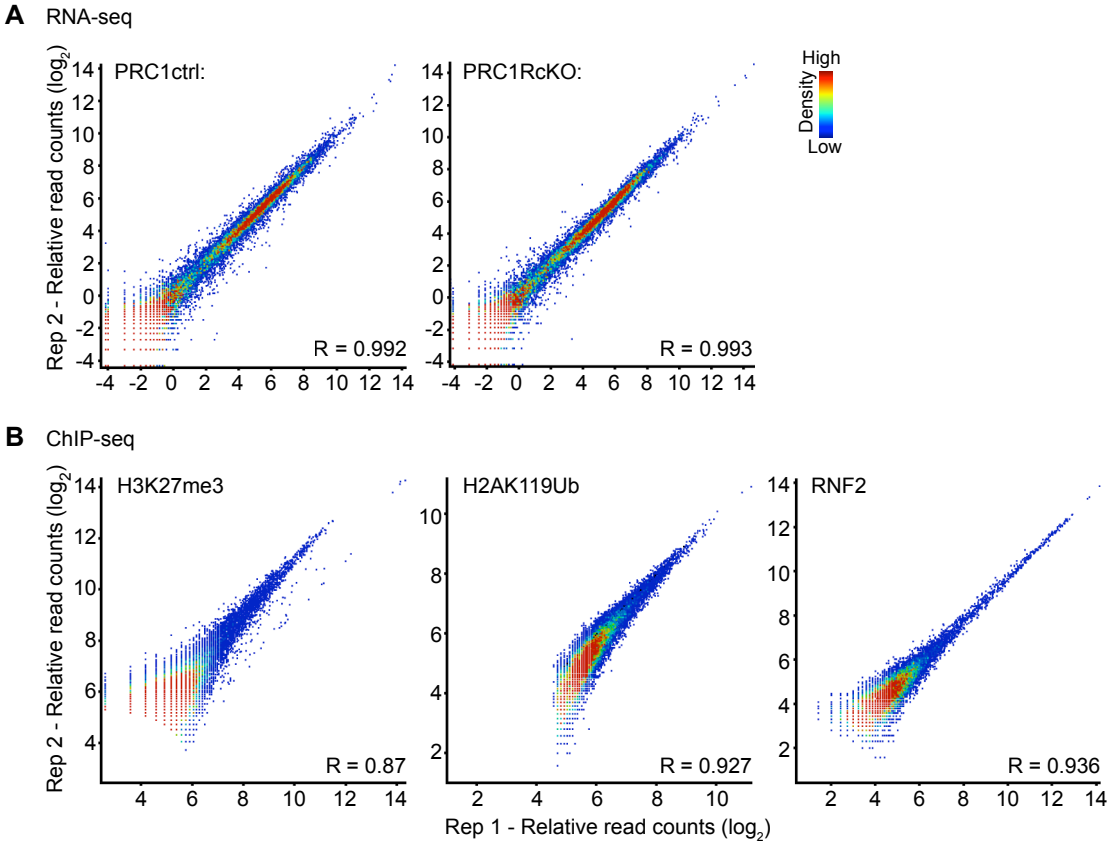

Figure 3- figure supplement 1. Biological replicates for RNA-seq and ChIP-seq data.
(**A**) Scatter plots show the reproducibility of RNA-seq enrichment at individual peaks between biological replicates. (**B**) Scatter plots show the reproducibility of and ChIP-seq enrichment at individual peaks between biological replicates. Each peak was identified using MACS ($P < 1\times10^{-5}$). H3K27ac ChIP-seq enrichment levels are shown in $\log_2$ RPKM values. The color scale indicates RNA-seq or ChIP-seq peak density. Pearson correlation values (R) are shown.

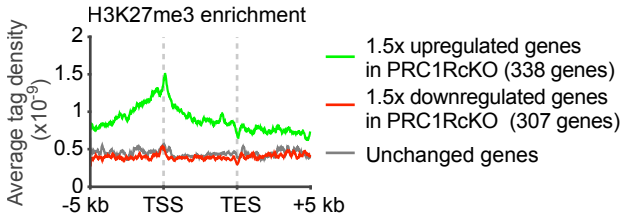

Figure 4- figure supplement 1. In Sertoli cells, H3K27me3 is enriched on genes required for granulosa cells. Average tag densities of H3K27me3 ChIP-seq enrichment on the groups of genes indicated in the panel.

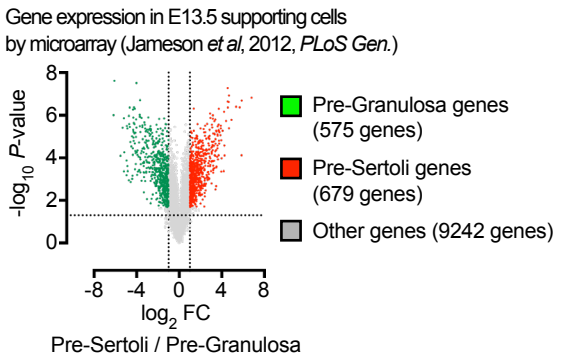

Figure 5- figure supplement 1. Expression profiles of specifically expressed genes in E13.5 granulosa cells. Microarray analysis of gene expression in E13.5 supporting cells (42). Genes with the criteria of 2-fold higher expression in E13.5 XX supporting cells and $P < 0.05$ were termed as "Pre-granulosa genes" and shown in green. Genes with the criteria of 2-fold higher expression in E13.5 XY supporting cells and $P < 0.05$ were termed as "Pre-Sertoli genes" and shown in red.

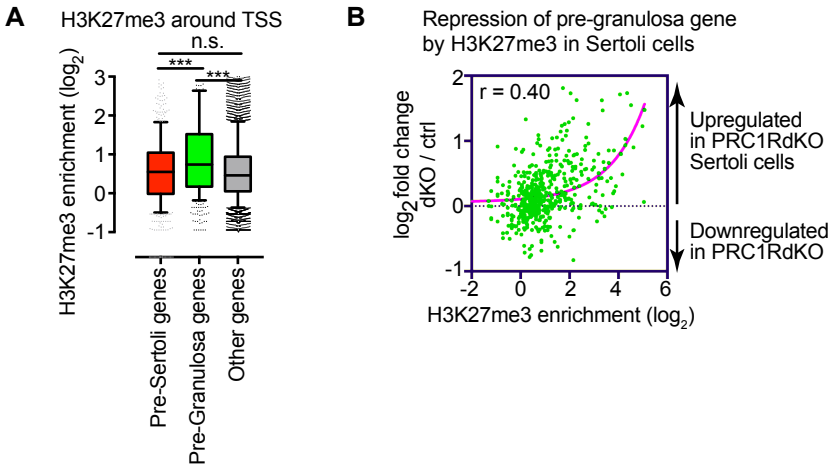

Figure 5- figure supplement 2. H3K27me3 is involved in the female gene regulatory network in Sertoli cells. (**A**) Box-and-whisker plots showing distributions of enrichment for H3K27me3 ChIP-seq data. Central bars represent medians, the boxes encompass 50% of the data points, and the whiskers indicate 90% of the data points. *** $P < 0.0001$, Mann-Whitney U tests. (**B**) Scatter plots showing the Pearson correlation between ChIP-seq enrichment (±2 kb around TSSs) and gene expression in Sertoli cells. A linear trendline is shown in blue.